

**Electro-sensing on Gold Surfaces in Order to Differentiate
Potassium and Ammonium Ions**

A Major Qualifying Project Report

Submitted to the Faculty

Of the

WORCESTER POLYTECHNIC INSTITUTE

In partial fulfillment of the requirements for the

Degree of Bachelor of Science in Chemistry

By

David Danico

Date: April 26, 2012

Approved:

Prof. Christopher Lambert, PhD, Advisor



Abstract

Ion selective electrodes are widely used in the biochemistry and biomedical fields where the measurements of ion concentrations in aqueous solutions are essential. The problem with these electrodes is accuracy; other ions interfering with the results of the measurements. This paper focuses on developing a more accurate ion selective electrode for potassium and ammonium ions. This was done by interacting 18-crown-6 ether on a gold surface with these ions and testing the electrochemical properties of these interactions. Potassium and ammonium ions have roughly the same shape and size as well as being the same charge and therefore are difficult to differentiate. In order to distinguish the two ions, an electrical current was applied to the electrochemical cell in the presence of a reductive agent thereby cleaving a hydrogen group from the ammonium ion. This changes the size, shape, and charge of ammonium and therefore changes the way it interacts with the 18-crown-6. With this technology, you are effectively increasing the accuracy of the ion selective electrode.

Table of Contents

Abstract	- 1 -
Table of Figures	- 3 -
Acknowledgements	- 5 -
Chapter 1: Introduction	- 6 -
1.1 Molecular Sensors	- 7 -
1.2 Self-Assembling Monolayers (SAMs)	- 9 -
1.3 Electrochemical Impedance Spectroscopy	- 11 -
1.4: Differentiating Ammonium (NH_4^+) and Potassium (K^+) Ions	- 12 -
Chapter 2: Instrumentation	- 14 -
2.1: Static Contact angle	- 15 -
2.2: Grazing Surface Infrared Spectroscopy	- 16 -
2.3 Cyclic Voltammetry	- 18 -
2.4 Impedance Spectroscopy	- 19 -
Chapter 3: Experimental	- 21 -
3.1: Synthesis of 4-mercapto-1-(1,4,7,10,13-pentaoxa-16-azacyclooctadecan-16-yl)butan-1-one: ...	- 22 -
3.2: Synthesis of 2-(6-mercaptohexyloxy)methyl-18-crown-6	- 23 -
3.2.1: First Step: Synthesis of 2-(6-bromohexyloxy)methyl-18-crown-6	- 23 -
3.2.2: Second Step: Synthesis of 2-(6-mercaptohexyloxy)methyl-18-crown-6	- 23 -
3.3: Preparation of 18-Crown-6 Self-Assembled Monolayers on Gold Surface	- 24 -
3.4: Preparation of COOH and NH_2 Thiol Self-Assembled Monolayers on Gold Surface	- 25 -
3.5: Characterization of Crown Ether SAMs	- 25 -
3.6: Electrochemical Impedance Spectroscopy	- 27 -
3.7: Ion Titrations	- 28 -
3.8: EIS of NH_2 and COOH Thiol Surfaces	- 30 -
3.9: CV of Potassium Ferricyanide	- 34 -
Chapter 4: Discussion	- 35 -
4.1: EIS Results and Discussion	- 36 -
4.2: Ion titrations Results and Discussion	- 36 -
4.3: EIS of NH_2 and COOH Thiol SAMs Results and Discussions	- 37 -
4.4: Difficulties and Recommendations for further study	- 38 -

Chapter 5: Conclusions	- 40 -
Appendix A: NMR Spectra.....	- 43 -
Appendix B: References	- 44 -

Table of Figures

Figure 1.1: Example structures of crown ether, aza-crown ether, and thia-crown ether; respectfully...-8-	-8-
Figure 1.2: 18-crown-6 ether bonded to a potassium ion.....-8-	-8-
Figure 1.3: A representation of the three basic components of SAMs.....-10-	-10-
Figure 1.4: Reaction of ammonia to an ammonium ion and vice versa.....-12-	-12-
Figure 2.1: Contact angle measurement and properties of SAM determined by Static Contact angle experiment.....-15-	-15-
Figure 2.2: Contact angle geometer.....-16-	-16-
Figure 2.3: Grazing Surface IR measurement.....-17-	-17-
Figure 2.4: IR active and inactive modes.....-17-	-17-
Figure 2.5: Sinusoidal Current Response in a Linear System.....-19-	-19-
Figure 3.1: Synthesis of 4-mercapto-1-(1,4,7,10,13-pentaoxa-16-azacyclooctadecan-16-yl) butan-1-one.....-22-	-22-
Figure 3.2: Synthesis of 2-(6-mercaptohexyloxy) methyl-18-crown-6.....-24-	-24-
Figure 3.3: IR spectrum of 2-(6-mercaptohexyloxy)methyl-18-crown-6 gold surface.....-26-	-26-
Figure 3.4: EIS Graph showing Z_{phz} of Potassium Ferricyanide redox solution at 200mV.....-28-	-28-
Figure 3.5: EIS Graph showing Z_{phz} of potassium ferricyanide solution at -150mV.....-28-	-28-
Figure 3.6: Titration graph of Ammonium ions in the presence of 5mM Potassium ions.....-29-	-29-
Figure 3.7: Potassium Titration in the presence of 5mM of Ammonium Ion.....-30-	-30-
Figure 3.8: Z_{phz} of NH ₂ and COOH thiol surface EIS with Potassium Ferricyanide as the redox probe.....-31-	-31-
Figure 3.9: Z_{mod} of NH ₂ and COOH thiol surface EIS with Potassium Ferricyanide as the redox probe.....-31-	-31-

Figure 3.10: Z_{phz} of NH ₂ and COOH thiol surface EIS with Hexaamineruthenium(III) Chloride as the redox probe.....	-31-
Figure 3.11: Z_{phz} of NH ₂ and COOH thiol surface EIS with Hexaamineruthenium(III) Chloride as the redox probe.....	-32-
Figure 3.12: Z_{phz} of NH ₂ and COOH thiol surfaces without a redox probe.....	-32-
Figure 3.13: Z_{mod} of NH ₂ and COOH thiol surfaces without a redox probe.....	-32-
Figure 3.14: Z_{phz} of COOH thiol surface EIS in the presence of 10mM NH ₄ ⁺ and Potassium ferricyanide redox probe.....	-32-
Figure 3.15: Z_{real} of COOH thiol surface EIS in the presence of 10mM NH ₄ ⁺ and Potassium ferricyanide redox probe.....	-32-
Figure 3.16: Z_{mod} of COOH thiol surface EIS in the presence of 10mM NH ₄ ⁺ and Potassium ferricyanide redox probe.....	-32-
Figure 3.17: CV graph of potassium ferricyanide solution.....	-34-
Figure 4.1: Differential Pulse Voltammetry Measurement.....	-39-

Acknowledgements

I would like to sincerely thank my advisor, Dr. Christopher Lambert, for the opportunity to work in his lab and complete this project. It has been an incredible learning experience and I thank you for the privilege. In addition, I would like to thank the faculty of the Chemistry and Biochemistry Department of WPI for providing a very valuable education and experience over the past four years.

I would also like to thank all the students in Christopher Lambert's Laboratory for being a tremendous help during the course of this project. Moreover I would like to specifically thank Morgan Stanton. With her vast knowledge and guidance, she has been an invaluable resource and I thank her for all her help.

Chapter 1: Introduction

1.1 Molecular Sensors

A molecular sensor (or chemosensor) is a molecule that interacts with an analyte to make a detectable change. These changes could include redox potentials, absorption, or fluorescence spectra. (Hewage, 2008) The term used to describe the use of molecular sensors in analytical chemistry is “Supramolecular Analytical Chemistry.” In the past few decades, supramolecular analytical chemistry (SAC) was focused of the use of molecular sensors to mimic biological receptors. In addition, one of the most promising areas of study using synthetic sensors in the area of deferential sensing. (Anslyn, 2007)

Crown ethers are one of the most studied parts of SAC. Crown ethers are macrocyclic compounds that contain $\text{CH}_2\text{-CH}_2\text{-O}$ groups. Many modified crown ethers have been developed including aza crowns and thia crowns (**Figure 1.1**). In 1982, a monograph recorded thousands of known structures and in 1993 another monograph was published describing the structures doubling that. It is estimated that there are over 10,000 crown ether molecules. (Gotkle et. al, 2004)

The property that makes crown ethers such an important part of supramolecular analytical chemistry is that it tends to bond to cations due to the ion-dipole interactions between the cation and the electron rich ring structure. (Hewage, 2008) The selectivity of these crown ethers depends on its ring size, the size of the cation, the charge of the cation, and the amount of electron donors of the crown ring. **Figure 1.2** shown below is a common example of a crown ether bonding a cation. In a study done by testing all the crown ethers from 12-crown-4 to 24-crown-8, it was determined that 18-crown-6 had the best bonding to the potassium ion. In addition, the 18-crown-6 ether also had a high affinity for bonding to Na^+ , Ca_2^+ , and NH_4^+ . (Gokel et al. 2004)

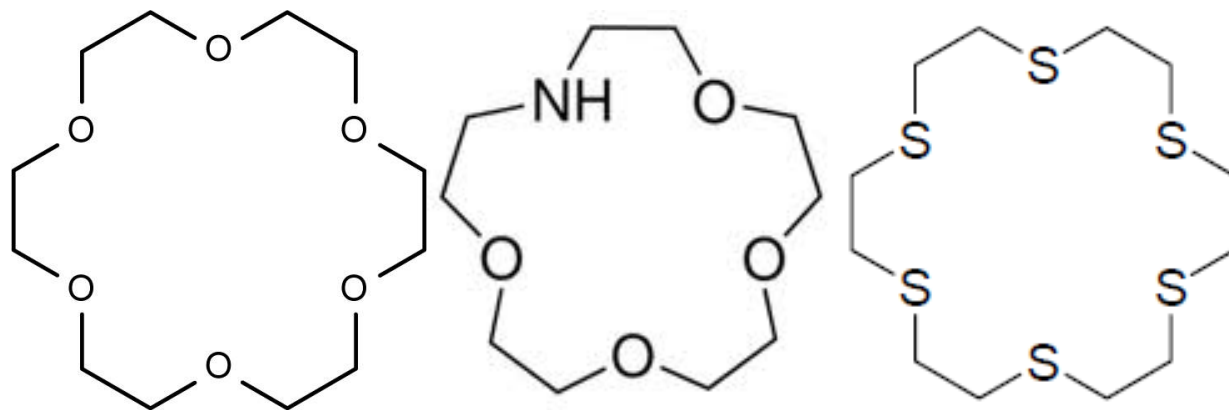


Figure 1.1: Example structures of crown ether, aza-crown ether, and thia-crown ether; respectfully.

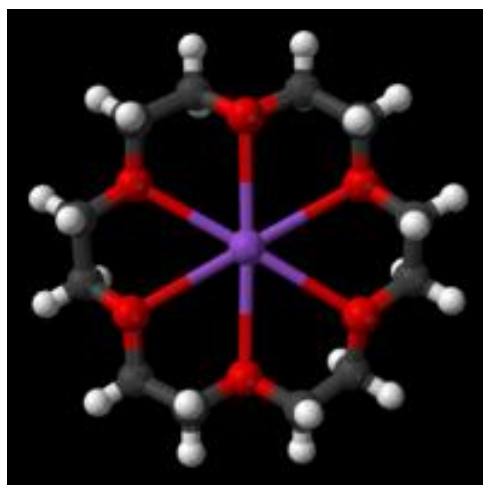


Figure 1.2: 18-crown-6 ether bonded to a potassium ion

1.2 Self-Assembling Monolayers (SAMs)

Self-Assembling Monolayers have received much attention over the past decade due to their ability to influence the physical properties of the exposed surface. Self-assembly describes a process in which a disorganized system of individual units organizes into an ordered system without any external impact. Overall, the free energy of the system decreases as the units organize. The forces behind self-assembly are van der Waals forces and hydrogen bonding. The macromolecular assembly is more thermodynamically stable than the unassembled arrangement through interactions between the individual components.

Work on self-assembling monolayers was first started in 1946 when Zisman first published the construction of a monomolecular layer by adsorption (self-assembly) of a surfactant (lowers surface tension of a liquid) onto a clean metal surface. (Bigelow, 1946) At this time the potential of SAMs was not fully understood and this publication did not reap the deserved attention; but as years went on and with publications such as by Nuzzo and Allara in 1983 which described that SAMs of alkanethiolates on gold could be prepared by immersion of di-n-alkyl disulfides from dilute solutions showed the possibilities of SAMs. (Nuzzo and Allara, 1983) (Ulman, 1996) Also in 1983, the first use of the term “self-assembling monolayers” was used in a work published in the *New Scientist* by Lucy Netzer and Jacob Sagiv with their work on absorption of silane surfactants on surfaces to generate oriented monolayers. (Netzer, 1983-1986) (New Scientist, 1983) Many self-assembling monolayers have been studied since then, but the most studied are alkanethiolates on gold surfaces.

Below is a diagram of the three basic molecular constituents of a SAM molecule (**Figure 1.3**); the head group, the tail, and the functional group. The head groups are usually thiols on gold. This is where the attachment chemistry happens. The tail is usually mostly

comprised of alkyl groups (CH₂) and this is where a great deal of the stability occurs as a result of chain to chain interactions (Van der Waals Forces). The functional groups of the self-assembling monolayer are used to control the properties of the metal substrate including wettability, biocompatibility, absorptivity, and molecular recognition. (Driscoll, 2009)

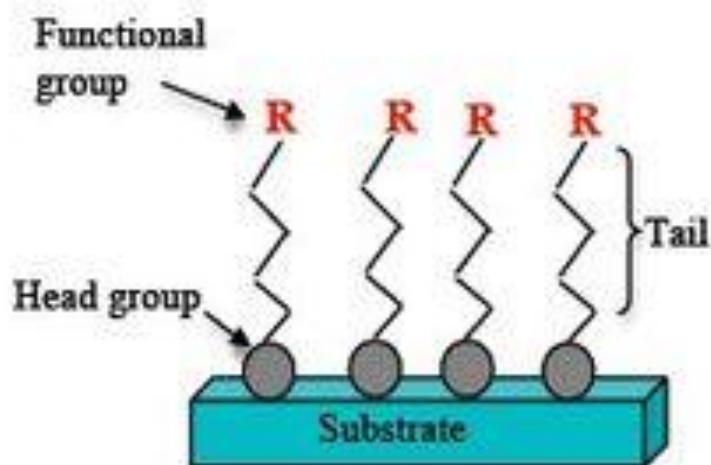


Figure 1.3: A representation of the three basic components of SAMs

Alkanethiols on gold surfaces are the most studied self-assembled monolayers. This is because the substrate and the thiol group both have their advantages. Gold does not easily oxidize, does not react with most chemicals, and is electrically conductive. Gold can also be easily thermally evaporated and placed on supports such as glass. Thin Gold slides can be characterized using many techniques including contact angle, cyclic voltammetry, electric impedance spectroscopy (EIS), and IR spectroscopy. (Sondag-Huethorst, 1995) Alkanethiols are very stable compounds and their synthetic procedures have been verified. Alkane thiols also have a high attraction to gold and easy form strong, durable bonds.

1.3 Electrochemical Impedance Spectroscopy

Electrochemical Impedance Spectroscopy (EIS) is a useful tool with applications including corrosion, biosensors, battery development, fuel cell development, paint characterization, sensor development, and physical electrochemistry. (Gamry Instruments, 2011) EIS is so powerful because it provides a potential and a current over a wide range of frequencies. EIS is based on making a disturbance in an electrochemical reaction from its steady state by applying a small excitation signal to the system. With this we can identify the electrochemical processes arising in the system. (Gryszakowski, 2011)

Impedance is a complex resistance encountered when electric current runs through a circuit made of resistors, capacitors, or inductors, or any grouping of these. Depending on how they are arranged, both the magnitude and phase shift of impedance can be determined. (Park, 2003) Impedance spectra is usually analyzed by fitting it to a model; called the equivalent circuit technique. In this technique, a simple circuit is assembled using the parts mention above and is applied to your data. The main disadvantage of this is that the model circuits don't have a uniqueness that is desired for each experiment; as stated by IUPAC, "It is definitely wrong to analyze experimental impedance data by just fitting it to an equivalent circuit corresponding to a trial and error. The reason for this is that the impedance response of several equivalent circuits can follow exactly the same function of frequency, only with different meanings of the corresponding elements. In addition, a fit will always be successful if an unlimited number of parameters is admitted. Without having a prior model, the meaning of these parameters is undefined." (Sluytersrehabach, 1994) The circuit model selected does not derive the system's physicochemical properties but is simply a likeness to the system. (Gryszakowski, 2011)

Electrochemical Impedance Spectroscopy is a technique used during the course of this project as a way to analyze the electrochemical properties of the 18-crown-6 thiol surface.

1.4: Differentiating Ammonium (NH₄⁺) and Potassium (K⁺) Ions

The objective of this project is to be able to tell the difference between ammonium and potassium ions in solution. Potassium and Ammonium ions have the same general shape and size as well as the same charge and therefore are very difficult to distinguish. To accomplish this, the electrochemical properties of the interaction between the ions and a SAM on a gold surface were observed by electrochemical impedance spectroscopy. The SAM used during the experiments was an 18-crown-6 ether with a thiol chain.

The main theory behind differentiating the two ions is that in the presence of a redox probe and at a certain potential, the ammonium ion would lose one of its hydrogen thereby making it a neutral substance (Ammonia) (**Figure 1.4**). In doing this, you are changing both the size and the shape of the ammonium ion and therefore changing the way it interacts with the 18-crown-6 SAM. Thus, at a certain potential, one would see a large difference in the impedance of the EIS measurement. With the large change in impedance, you are affectively showing a difference between the two ions.

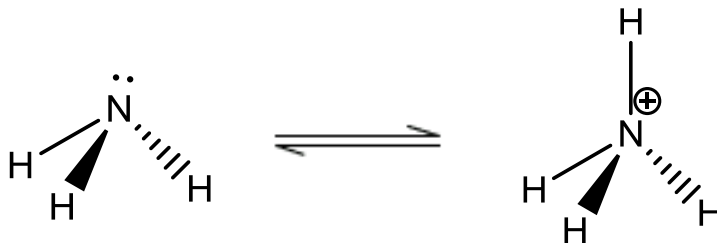


Figure 1.4: reaction of ammonia to an ammonium ion and vice versa.

To be able to differentiate the two ions, a sensor was made with the components of the 18-crown-six thiol ether and a gold surface. EIS measurements were used to test how the potassium and ammonium ions interact with the gold surface. Currently there are ways to detect potassium ions, but the problem with these probes is that in the presence of a relatively small concentration of ammonium ions, the data produced becomes inaccurate. With the application of a current, the gold surface would become more accurate in the differentiation of the potassium and ammonium ions.

Chapter 2: Instrumentation

This chapter aims to give a look into some of the experimental techniques used during the course of this project. Techniques used in this paper include: static contact angle, infrared spectroscopy, cyclic voltammetry, and electrochemical impedance spectroscopy.

2.1: Static Contact angle

The static contact angle technique entails a drop of liquid, usually water, placed on a surface to be analyzed. Then the angle the liquid makes with the surface is measured. Non polar terminal groups of SAMs tend to make the surface hydrophobic causing the contact angle to be high (>90). An example of this type of SAM is dodecanethiol, which has a contact angle of 112° . If the terminal group is polar, than the surface tends to be more hydrophilic resulting in a low contact angle (<90). An example of this would be the carboxylic acid groups of mercaptoundecanoic acid which have a contact angle around 29° . (Driscoll, 2009) **Figure 2.1** shows measurements of hydrophilic and hydrophobic measurements and the properties that go with them. **Figure 2.2** shows a picture of the instrument used to measure the static contact angles. This machine consists of a light source, a camera, a movable stage, and a liquid dispenser.

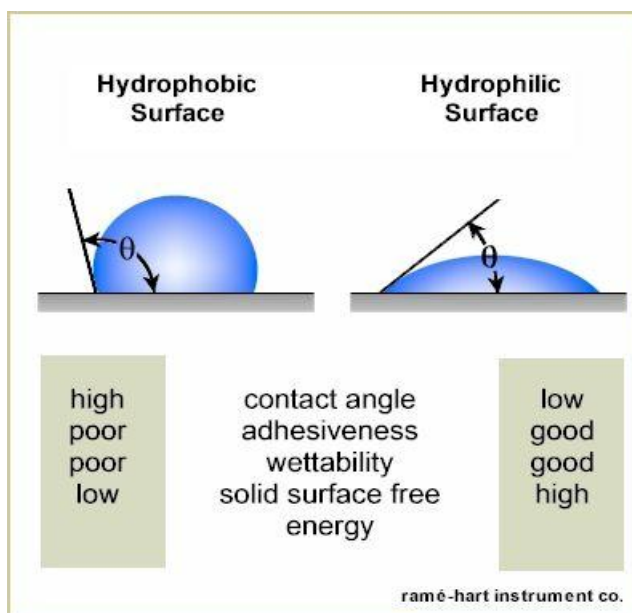


Figure 2.1: Contact angle measurement and properties of SAM determined by Static Contact angle experiment

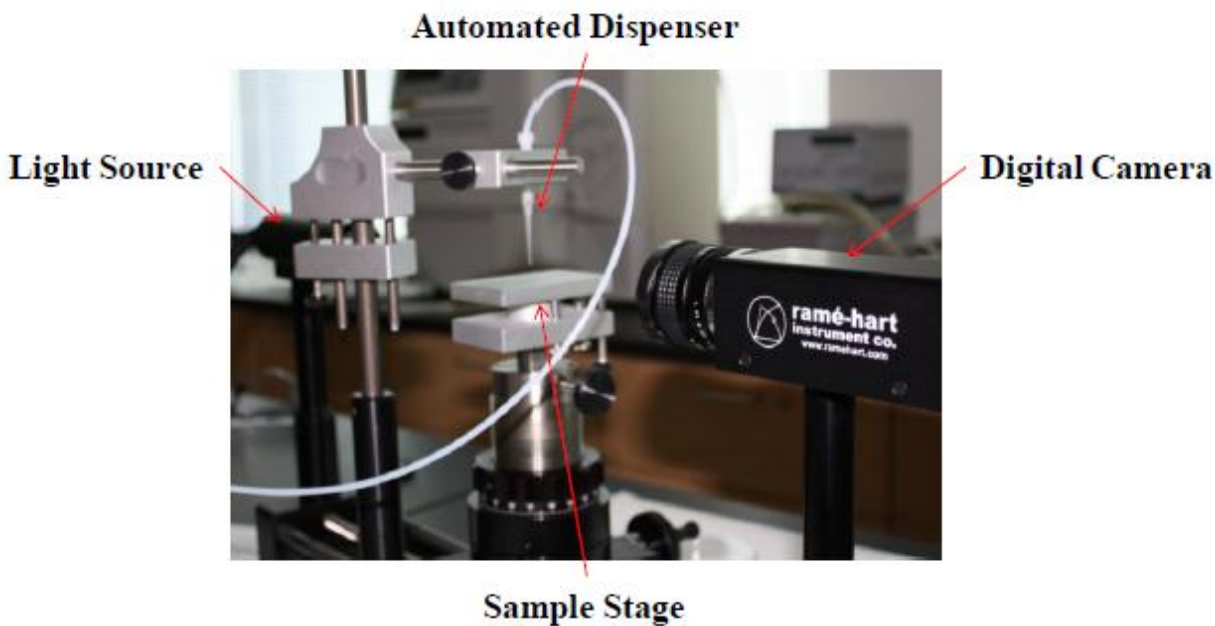


Figure 2.2: Contact angle geometer (Driscoll, 2009)

2.2: Grazing Surface Infrared Spectroscopy

Grazing surface infrared spectroscopy is a way of analyzing the functional groups of the monolayer on a surface. As the spectrometer starts the experiment, an infrared (IR) beam is reflected off the monolayer surface and the intensity of the beam is detected on the other side (**figure 2.3**). The grazing angle at which the beam hits the surface increases the sensitivity of the measurement. In addition, nitrogen is spayed into the area of measurement thereby clearing away any water particles or other particles that might affect the measurement which also increases sensitivity. Not all absorption bands in a monolayer are present in an IR spectrum. This is due to the positioning of the bonds comparative to the surface. Only the vibrations that have the dipole perpendicular to the surface are seen. Molecules on a metal surface induce a local opposite charge on the substrate which enhances the transition dipoles when it is perpendicular and suppresses them when it's parallel (**figure 2.4**). (Driscoll, 2009)

Figure 2.3: Grazing Surface IR measurement

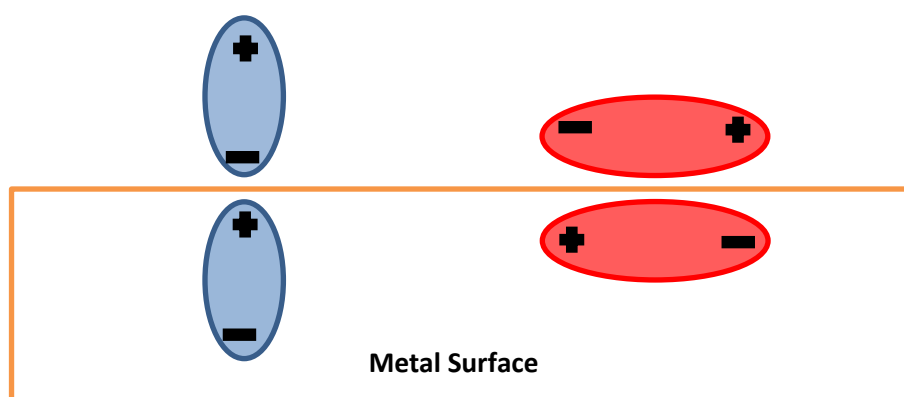
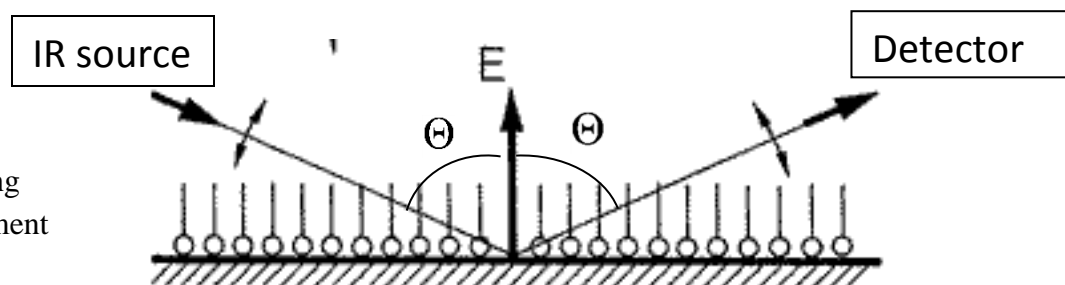


Figure 2.4: IR **active** and **inactive** modes

IR spectra were taken with a Nexus 870 FT-IR and Omnic Version 7.2 software. The angle of IR beam was set at 75° . The spectrometer was purged with nitrogen for 30 minutes prior to experimentation and continued during the experiment. The background was taken with a Piranha cleaned gold slide and background was taken before each IR measurement. The spectra were automatically corrected for H₂O and CO₂, and a manual baseline correction was completed after each experiment.

2.3 Cyclic Voltammetry

Cyclic voltammetry (CV) is used to examine a self-assembled monolayer's ability to transfer electrons. This process involves changing the potential across two electrodes and measuring the ensuing current. If a redox species is present, then you would see peaks in the anodic and cathodic currents which represent oxidation and reduction respectively. CV measurements are made to test the blocking nature of the SAM on the surface being tested during this redox process. If the SAM is well ordered it forms an insulating layer over the surface resulting in a decrease of the redox process. (Andrienko, 2008)

The working electrode for these experiments is a gold slide and electron flow goes from the working electrode to the counter electrode (platinum wire). The potential is measured between the reference electrode (electrode with known, constant potential) and the working electrode. A redox species is used as well as an electrolyte to help carry the charge and the cell containing the three probes is connected to the potentiostat which manages the potentials running through the cell. (Andrienko, 2008) An example of a CV measurement using a blank gold slide, and a redox probe (ferricyanide) is shown in **figure 3.17** in the next chapter.

CV was run using a Gamry Instruments Reference 600 Potentiostat/Galvanostat/ZRA. A three probe cell was used with a gold slide as the working electrode, platinum wire as the counter electrode, and Ag/AgCl reference electrode. The surface area of the working electrode placed in the electrolyte solution was 1 cm^2 . Voltammograms were attained from -0.5 V to 0.5 V with a scan rate of 50 mV/s. The redox potential was determined by taking the average potentials at the maximum peak and the minimum peak.

2.4 Impedance Spectroscopy

Electronic Impedance Spectroscopy is usually measured by applying an electrical potential to an electrochemical cell and measuring the current. If one were to apply a sinusoidal potential to the cell the response would be the AC current signal. EIS is normally measured using an excitation signal that makes the cell respond pseudo-linearly. With this linear system, the current response of the sinusoidal potential will be a sinusoid (curve described by the equation $y = a \sin[x]$) at the same frequency but with a shift in phase. (Gamry Instruments, 2010)

Figure 2.5 shows this system. The two lines represent the current and voltage of the electrochemical cell. Therefore, when doing EIS, you are measuring the amplitudes of both the voltage and current, and measuring the distance between these peaks; the phase shift. With these variables measured, the impedance (Z) of the system is determined by **equation 1** with the V representing voltage, I representing current, f representing the frequency, and Φ representing the phase shift. For a resistive element the impedance is independent of frequency and the measured current is in phase with the AC perturbations voltage. For a pure capacitor, the current is out of phase with the voltage and is frequency dependent.

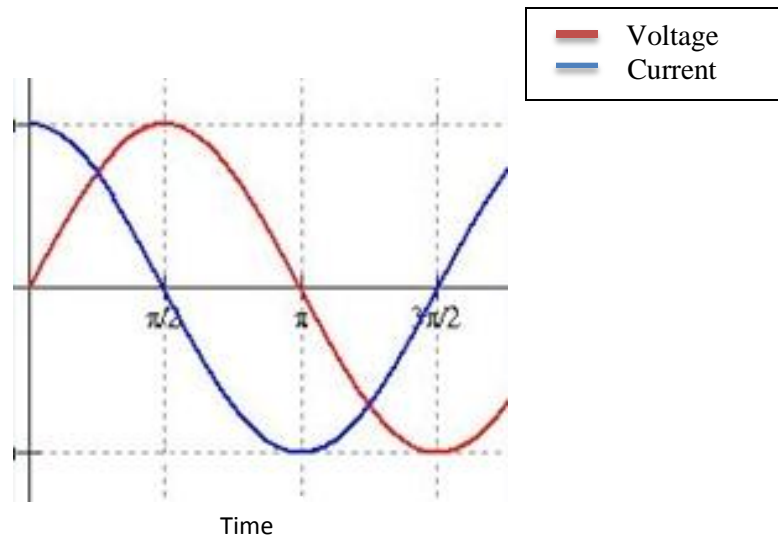


Figure 2.5: Sinusoidal Current Response in a Linear System

$$Z = |Z| \cdot e^{j\phi} = Z' + j \cdot Z'' = \frac{V \sin(2\pi f)}{I \sin(2\pi f + \phi)} \quad (1)$$

EIS was done in the same way as described for cyclic voltammetry with the same electrode set up consisting of a working, counter, and reference electrode. Tetra-n-butylammonium chloride (0.1 M) was used in addition to a redox probe (1mM) (Potassium Ferricyanide or hexammineruthenium(III) chloride) to make an electrolyte solution for the ions being tested. Measurements were taken from -500 to 500 mV with frequencies ranging from 100000 Hz to 0.1 Hz (5 points decade) and Gamry Echem Analyst (v.5.50) software was used to analyze the data collected.

Chapter 3: Experimental

3.1: Synthesis of 4-mercapto-1-(1,4,7,10,13-pentaoxa-16-azacyclooctadecan-16-yl)butan-1-

one:

A solution was made by combining 1-aza-18-crown-6 (1.0 g, 3.8 mmol), 1.2 equivalents of γ -thiobutyrolactone (0.3463 mL, 4.0 mmol), and camphorsulfonic acid (0.1765 mmol) in toluene (3mL). This solution was heated to 100°C for 18 hours in an atmosphere of nitrogen and under reflux. The solution was then washed with aqueous sodium bicarbonate and water in triplicate while saving the organic phase. The organic phase was dried over magnesium sulfate and excess solvent was removed by rotary evaporation. The crude product was then purified by silica gel chromatography using a solution of dichloromethane/methanol (50:1). Fractions of the effluent that contained the pure product were identified by TLC and combined together. The solvent was removed by rotary evaporation resulting in a pale yellow oil. Yield 0.079 g (7.9%). $^1\text{H-NMR}$ (CDCl_3) δ (ppm): 3.44-3.39 (multiplet, 24 H crown), 2.42-2.39 (quartet, 2H CH_2), 2.33-2.30 (triplet, 2H CH_2), 1.78-1.73 (pentet, 2H CH_2), 1.16-1.13 (triplet, 1H SH). (Yang et al., 2000)

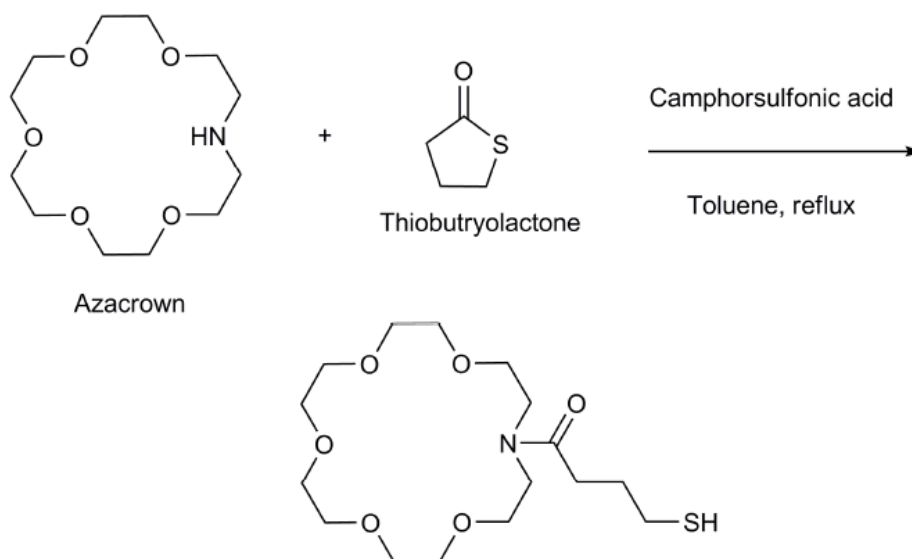


Figure 3.1: Synthesis of 4-mercapto-1-(1,4,7,10,13-pentaoxa-16-azacyclooctadecan-16-yl)butan-1-one:

3.2: Synthesis of 2-(6-mercaptohexyloxy)methyl-18-crown-6

This synthesis is done in a two-step process which is listed below. (Flink, 1999)

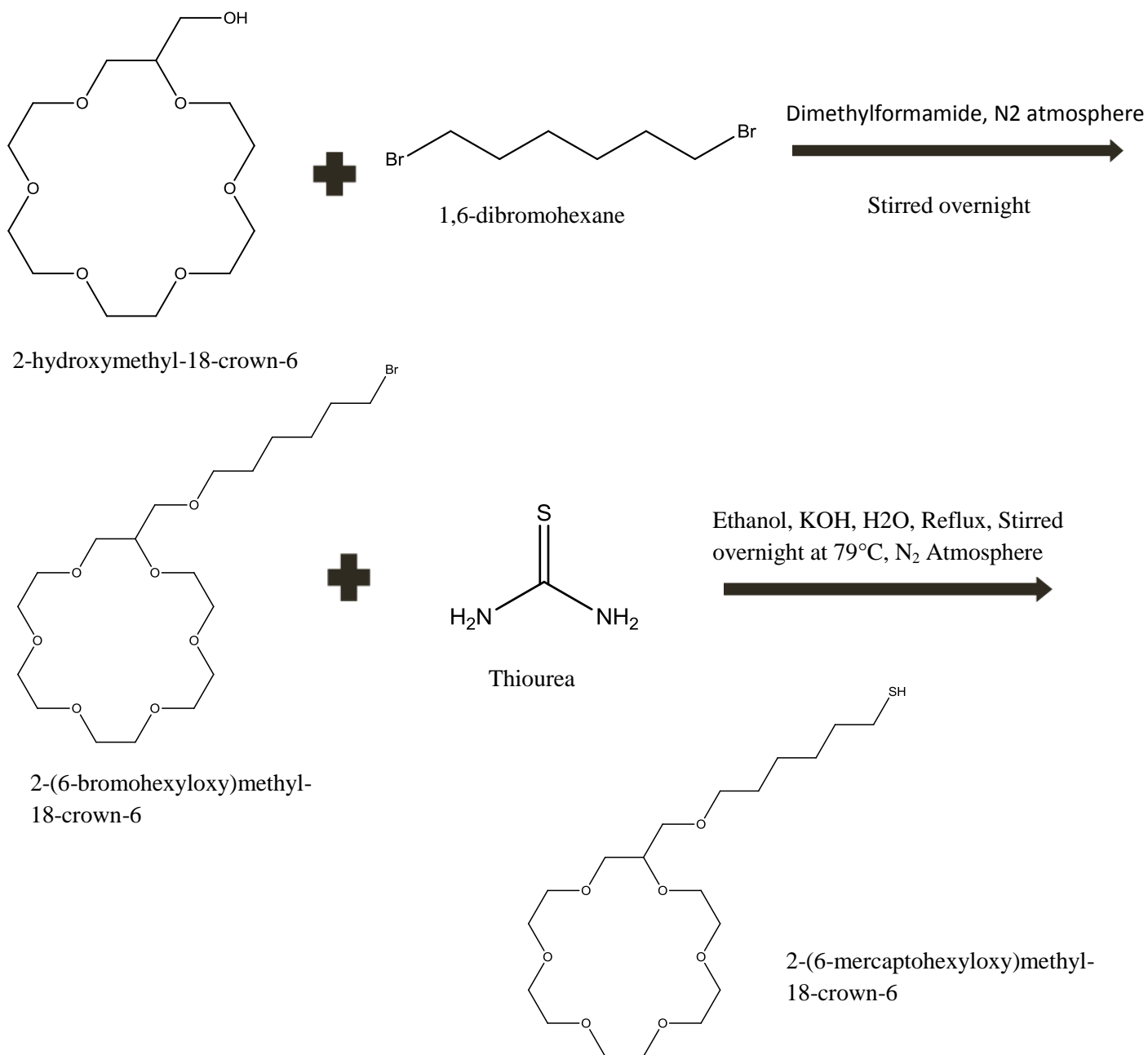
3.2.1: First Step: Synthesis of 2-(6-bromohexyloxy)methyl-18-crown-6

A solution was made with 2-hydroxymethyl-18-crown-6 (2 g, ~7mmol), N,N-Dimethylformamide (100mL), and sodium hydride (0.5g) (57%-63% oil dispersion). This mixture was stirred at room temp for 30 minutes, then 1,6-dibromohexane was added. The solution was stirred overnight and then quenched with methanol (100mL). Solution was concentrated in a vacuum and oil was taken up with Dichloromethane (100mL), washed 3x with water and dried with MgSO₄. Solvent was evaporated and purified using Al₂O₃ column (eluent hexane to ethyl acetate) which yields yellow oil (1.921g, 62%). ¹H-NMR (CDCl₃) δ (ppm): 1.28-1.50 (m, 4H), 1.50-1.65 (m, 2H), 1.80-1.92 (m, 2H), 3.35-3.50 (m, 6H), 3.55-3.85 (m, 23H)

3.2.2: Second Step: Synthesis of 2-(6-mercaptohexyloxy)methyl-18-crown-6

Purified 2-(6-bromohexyloxy)methyl-18-crown-6 (1.921g) and Thiourea (0.64g, 8.4mmol) were dissolved in ethanol (60mL) and heated under reflux and nitrogen atmosphere for 20 hours at a temp of 79°C. Potassium hydroxide (0.31g, 5.53mmol) and nitrogen purged water was added. This mixture was heated under reflux for 2 hours. The solution was then acidified with 1M perchloric acid (50mL). The aqueous layer was extracted with dichloromethane (3x100mL), dried over MgSO₄, filtered, and solvent removed by roto evaporation. The oil was purified using an Al₂O₃ Column (eluent hexane to ethyl acetate) yielding a colorless oil (0.43g, 25%). ¹H-NMR (CDCl₃) δ (ppm): 1.48-1.70 (m, 4H), 2.51 (dt, 2H), 3.35-3.55 (m, 4H), 3.56-3.85 (m, 23H)

Figure 3.2: Synthesis of 2-(6-mercaptohexyloxy)methyl-18-crown-6



3.3: Preparation of 18-Crown-6 Self-Assembled Monolayers on Gold Surface

Preceding the adhesion of the self-assembled monolayer (SAM) on gold surfaces, gold slides were cut into 2 cm x 1cm rectangles. After, the slides were cleaned, first in a

Piranha solution (30 % NaOH and 70% Sulfuric acid) for 10 minutes and then cleaned with oxygen plasma for 45 seconds. When the plasma cleaning was complete, the gold slides were immediately put into the thiol SAM solution which consisted of the 2-(6-Mercaptohexyloxy)methyl-18-crown-6 (1mM) in ethanol. The solution was left overnight. The new crown thiol gold surfaces were then rinsed with ethanol and dried in a nitrogen stream. The slides were stored in a clean parafilm pitri dish at $\sim 3^{\circ}\text{C}$ until experimentation.

3.4: Preparation of COOH and NH₂ Thiol Self-Assembled Monolayers on Gold Surface

Gold slides were cut into 1x2 cm strips then piranha cleaned (3:7 hydrogen peroxide to sulfuric acid). The ethanolic SAM solution for the COOH thiol was made with ethanol, 11-mercaptoundecanoic acid (0.5 mM), and 2% (v/v) of CF₃COOH. The ethanolic SAM solution for the NH₂ thiol was made with ethanol, 11-amino-1-undecanethiol (0.5 mM), and 3% (v/v) N(CH₂CH₃)₃. The Piranha cleaned gold slides were then oxygen plasma cleaned for 60 seconds then immediately placed into the SAM solutions and left over night. The COOH and NH₂ SAM surfaces were then rinsed with ethanolic solutions of ethanol and 10% NH₄OH (for COOH thiol) and ethanol and 10% (v/v) CH₃COOH (for NH₂ thiol). Then the gold slides were rinsed with pure ethanol and dried in a stream of nitrogen gas. The thiol gold surfaces were placed in parafilm pitri dishes and stored at $\sim 3^{\circ}\text{C}$ until needed for experimentation. The Contact angles for the COOH thiol surface was $20.8^{\circ} \pm 2.5^{\circ}$ and for the NH₂ thiol surface was $62.7^{\circ} \pm 6.3^{\circ}$. (Wang et. al, 2005)

3.5: Characterization of Crown Ether SAMs

The crown ether gold slides were characterized using static contact angle and grazing surface infra-red spectroscopy. The average contact angle of all slides tested was 56.04° . This contact angle is in conformity with other known values of similar films. (Flink et.

al,1998)(Flink et. al,1999) A basic example of a contact angle measurement was shown in the last chapter (**Figure 2.1**) and the characteristics of a hydrophobic and a hydrophilic measurement are listed.

The Grazing IR spectra for the 18-crown-6 thiol is shown in **figure 3.3**.

Absorptions include: $\sim 1127\text{ cm}^{-1}$ representing the C-O stretching of the ether groups, $\sim 2877\text{ cm}^{-1}$ and $\sim 2900\text{ cm}^{-1}$ represent the symmetric and asymmetric CH_2 stretching vibrations of the crown ether ring and alkyl chain. The observation of the C-H stretches of the chain at $\sim 2900\text{ cm}^{-1}$ and $\sim 2877\text{ cm}^{-1}$ for the surface is indicative of a slightly disorganized, liquid-like arrangement of the molecules, expected due to the short chain length and bulky head group. This is similar to reports that discuss SAMs containing crown ether. (Flink,1998)(Flink,1999)

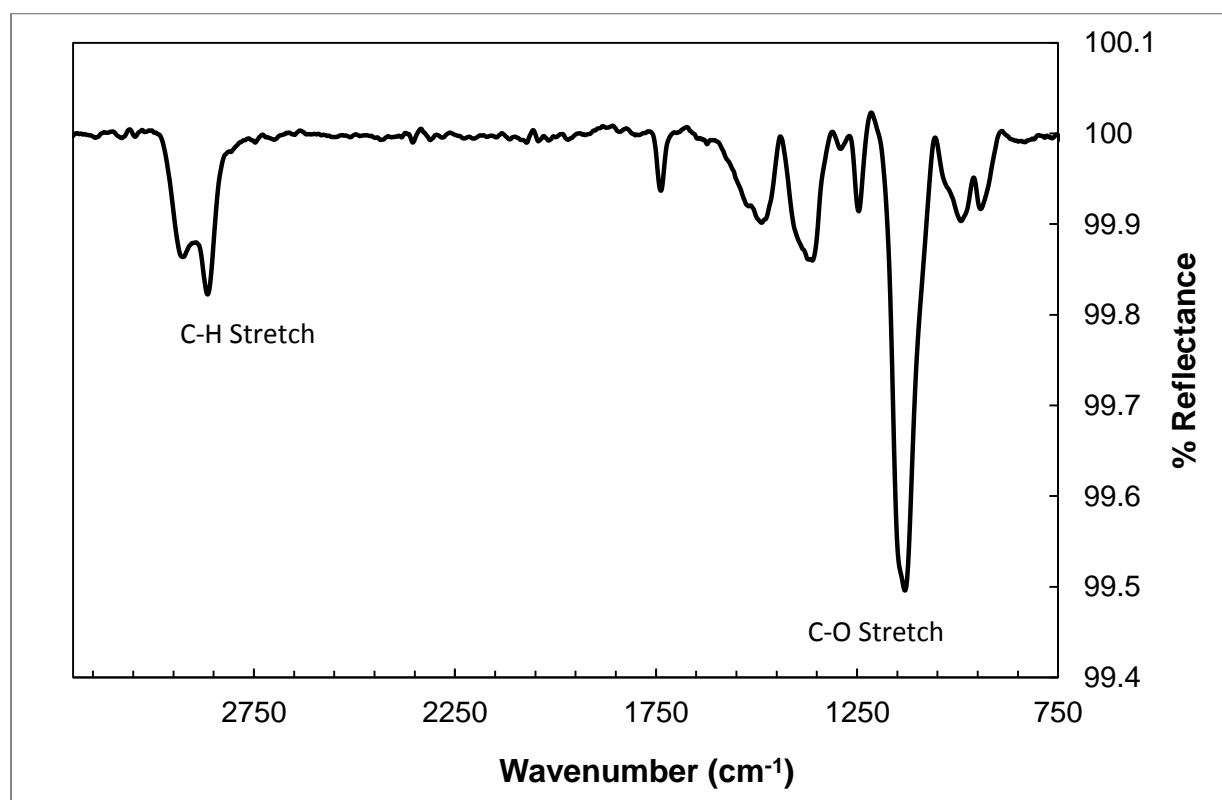


Figure 3.3: IR spectrum of 2-(6-mercaptohexyloxy)methyl-18-crown-6 gold surface

3.6: Electrochemical Impedance Spectroscopy

Electrochemistry Impedance spectroscopy (EIS) was used to find the frequency and the potential needed to differentiate between the potassium ions and the ammonium ions. The potentiostat requires an electrochemical cell with three electrodes; these electrodes being a working electrode, a reference electrode, and a counter electrode. The electrodes used for the following experiments were a gold slide with the crown thiol surface as the working electrode, Silver/Silver Chloride (Ag/AgCl) as the reference electrode, and a platinum wire as the counter electrode. The amount of surface area of the working electrode exposed to the solution was 1cm^2 .

For the EIS experiments a solution of tetra-n-butyl ammonium chloride (0.1 M) and hexamineruthenium(III) chloride (0.001 M), as the redox probe, was used along with the ion being tested for. A potassium chloride (0.01 M) solution, an ammonium chloride (0.01 M) solution, and a blank (neither potassium nor ammonium ions present) solution were made. To consider which frequencies and potentials provided the greatest separation, solutions were tested with frequencies that ranged from 100000 Hz to 0.1 Hz and with potentials that ranged from -500mV to 500mV; increasing in increments of 50mV.

This experiment was also done with potassium ferricyanide (0.001 M) as the redox probe and once again with no redox probe. The Z_{phase} , Z_{real} , $Z_{\text{imaginary}}$, and Z_{mod} of each solution were compared at each potential.

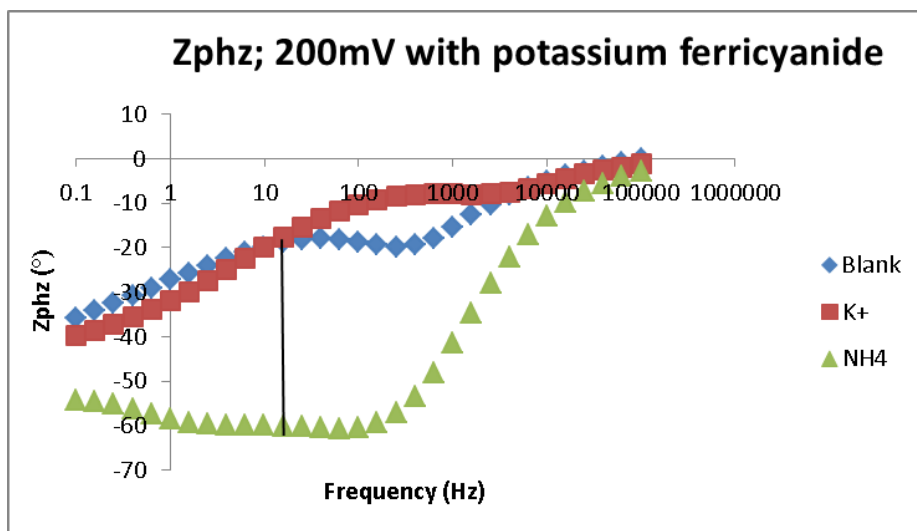


Figure 3.4: EIS Graph showing Z_{phz} of Potassium Ferricyanide redox solution at 200mV

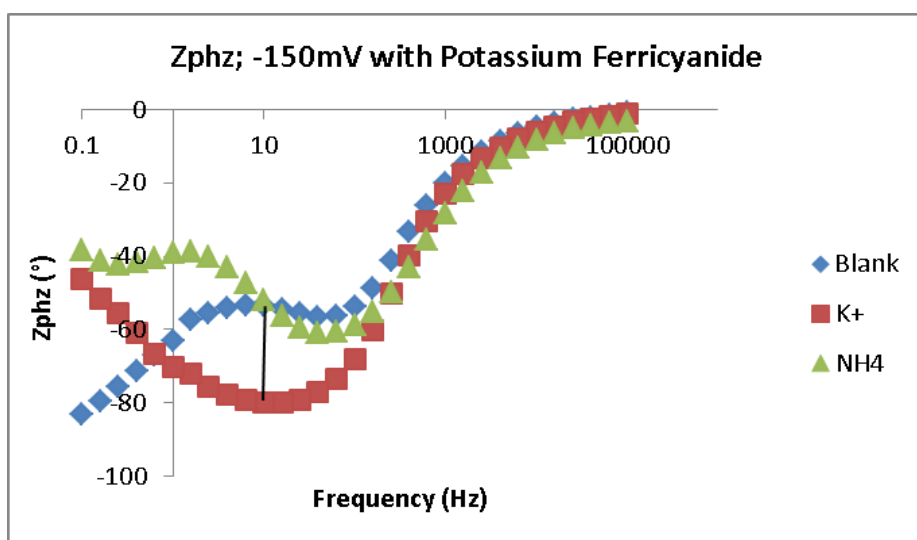


Figure 3.5: EIS Graph showing Z_{phz} of potassium ferricyanide solution at -150mV

3.7: Ion Titrations

Ion titrations were completed by adding small amounts of ion (K^+ or NH_4^+) to the supporting salt solution and redox probe. In this case the redox probe was potassium ferricyanide (1 mM) and the salt solution was tetra-n-butylammonium chloride (0.1 M). The concentration of ion in solution ranged from 0 mM to 10 mM and this was done in the presence of the other ion (5 mM). These measurements were done with a planer 1cm^2 gold slide that contained the 18-crown-6 thiol SAM. The titration was monitored by impedance spectroscopy

and the Z_{phz} at each concentration was examined. **Figure 3.6** and **Figure 3.7** show the results for these experiments. As you can see, these titrations go against what was predicted by **Figures 3.4** and **3.5**. The Z_{phz} for each titration should have become more negative as the concentration of the ions increased but both became more positive.

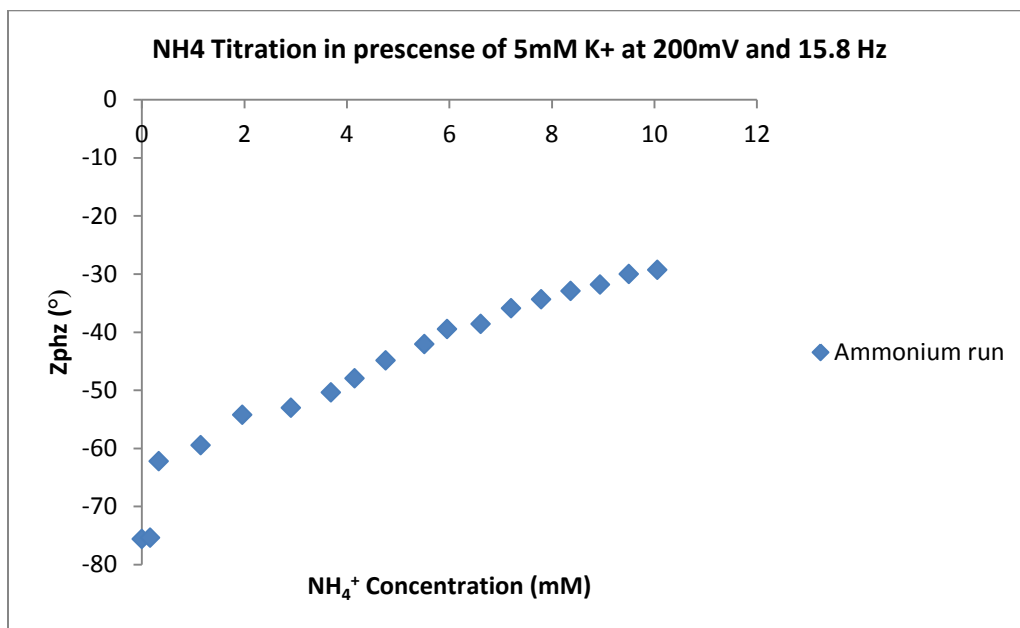


Figure 3.6: Titration graph of Ammonium ions in the presence of 5mM Potassium ions

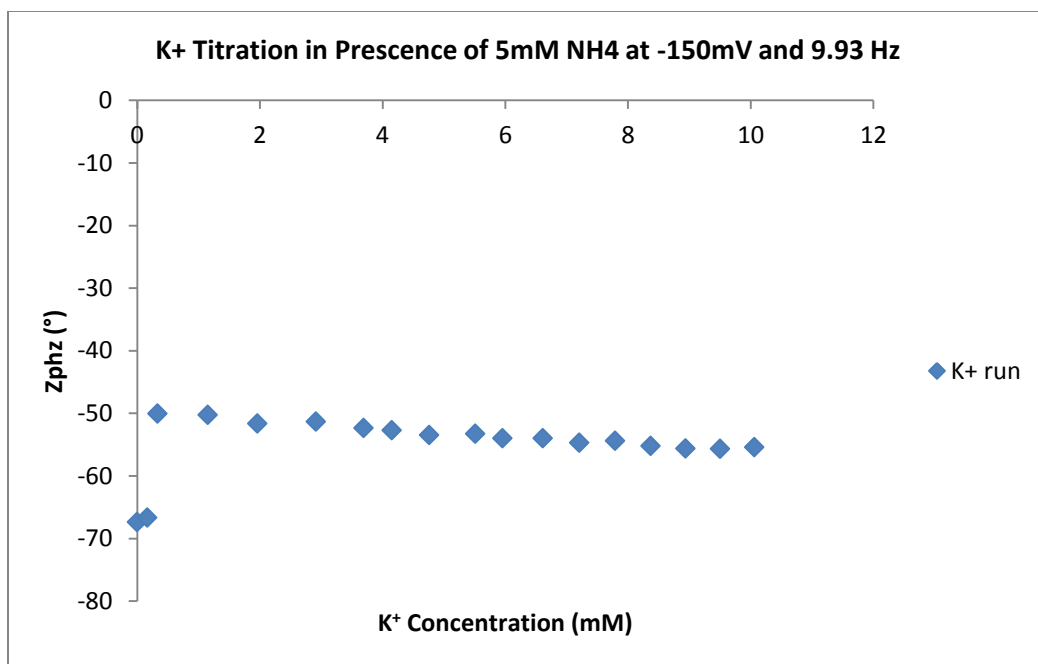


Figure 3.7: Potassium Titration in the presence of 5mM of Ammonium Ion

3.8: EIS of NH₂ and COOH Thiol Surfaces

EIS measurements were done on gold slides with surfaces of COOH thiol and NH₂ thiol. Solutions were made with tetra-n-butylammonium chloride (.1 M) and a redox probe (0.001 M). Three solutions were made for each thiol surface; a solution with potassium ferricyanide as the redox probe, a solution with hexamineruthenium(III) chloride as the redox probe and another with no redox probe. Measurements were taken at potentials -500mV to 500mV increasing by 50mV and at a range of frequencies from 100000 Hz to 1 Hz. In addition, The COOH thiol surface was tested in the presence of 10mM ammonium chloride. The Z_{phase} , Z_{mod} , and Z_{real} of each solution were analyzed at 15.84Hz (**figures 3.8-3.16**).

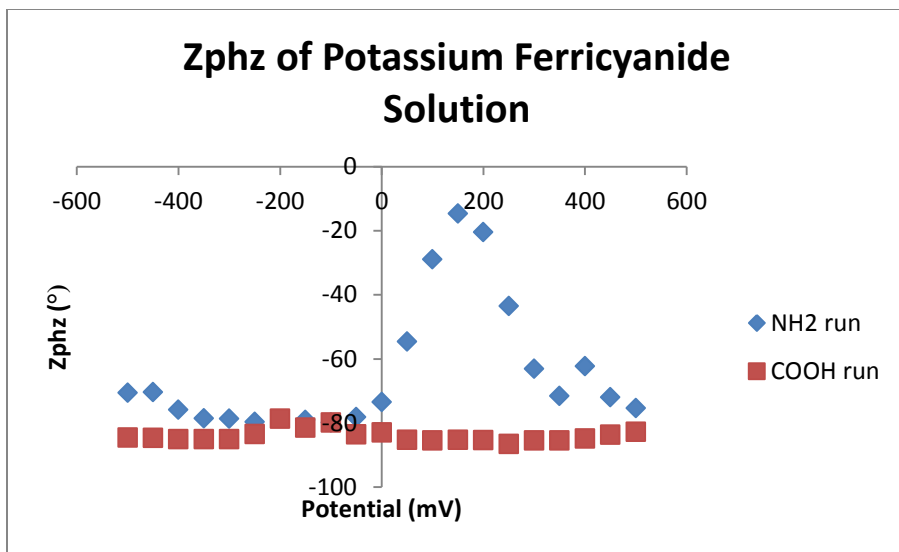


Figure 3.8: Z_{phz} of NH_2 and $COOH$ thiol surface EIS with Potassium Ferricyanide as the redox probe

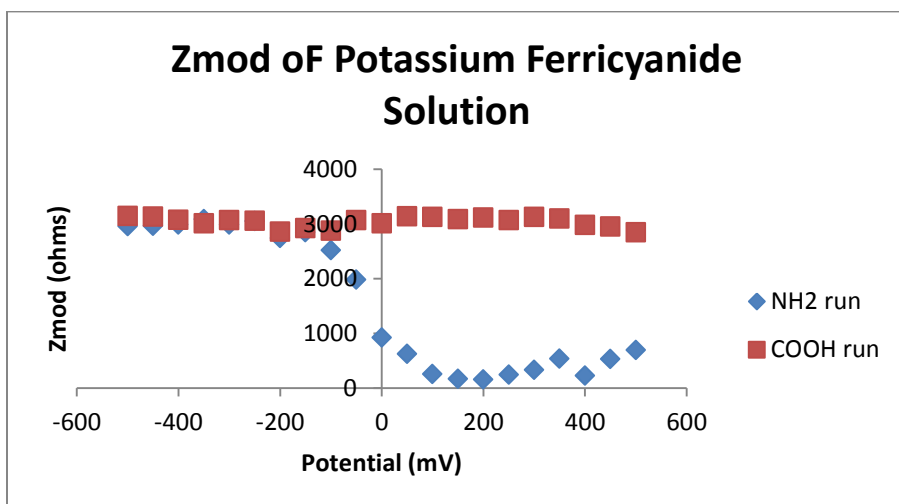


Figure 3.9: Z_{mod} of NH_2 and $COOH$ thiol surface EIS with Potassium Ferricyanide as the redox probe

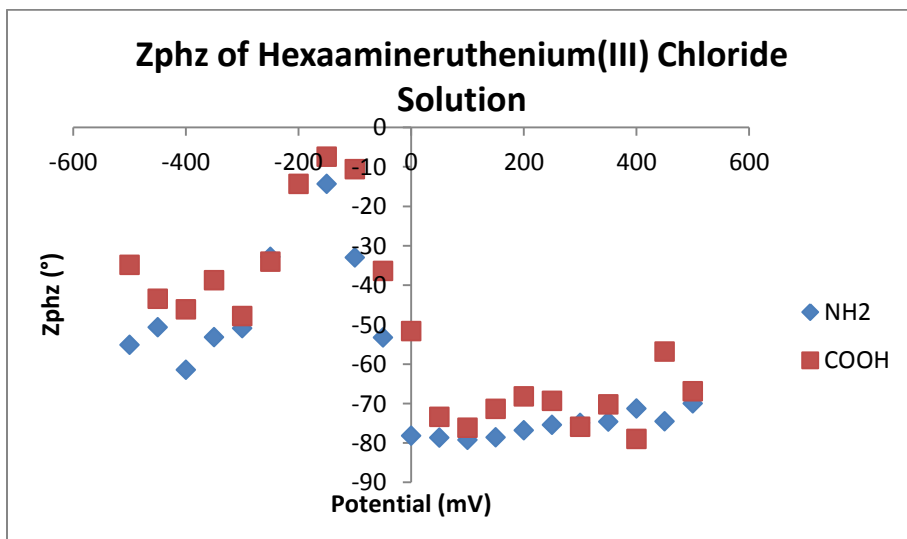


Figure 3.10: Z_{phz} of NH_2 and $COOH$ thiol surface EIS with Hexaamineruthenium(III) Chloride as the redox probe

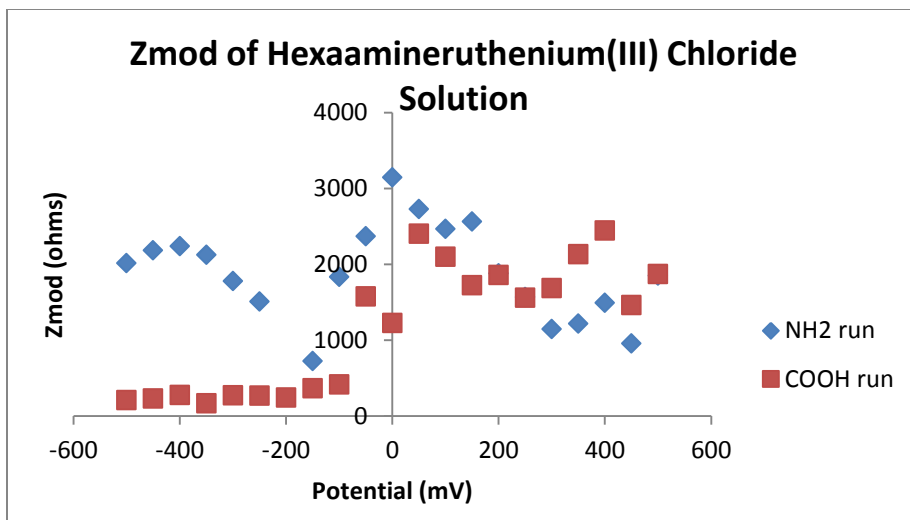


Figure 3.11: Z_{phz} of NH_2 and $COOH$ thiol surface EIS with Hexaamineruthenium(III) Chloride as the redox probe

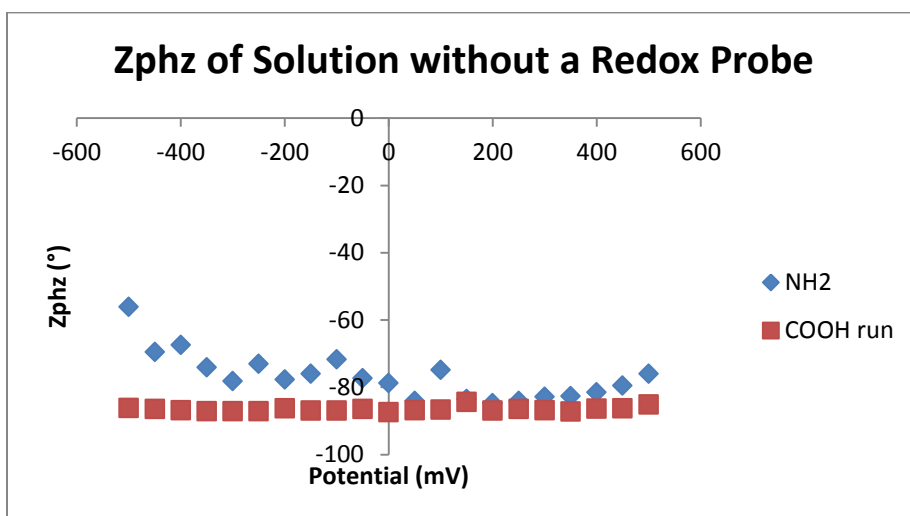


Figure 3.12: Z_{phz} of NH_2 and $COOH$ thiol surfaces without a redox probe

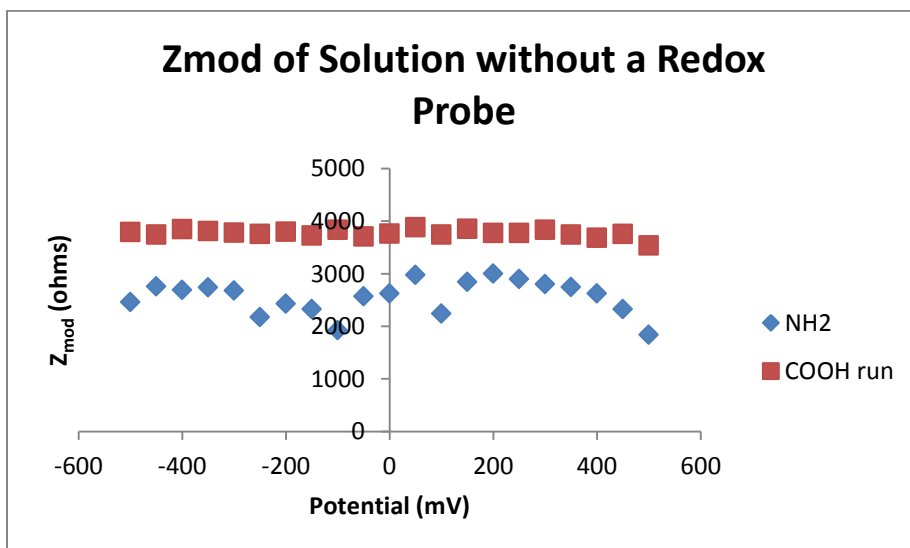


Figure 3.13: Z_{mod} of NH_2 and $COOH$ thiol surfaces without a redox probe

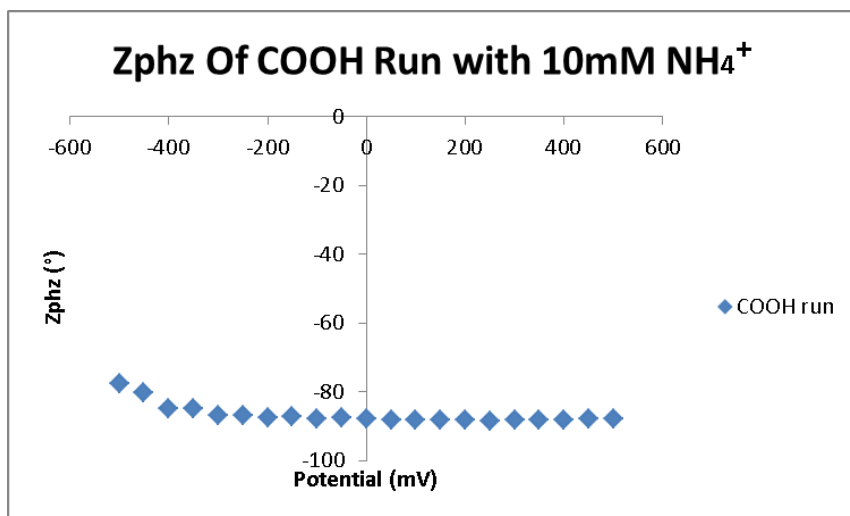


Figure 3.14: Z_{phz} of COOH thiol surface EIS in the presence of 10mM NH_4^+ and Potassium ferricyanide redox probe

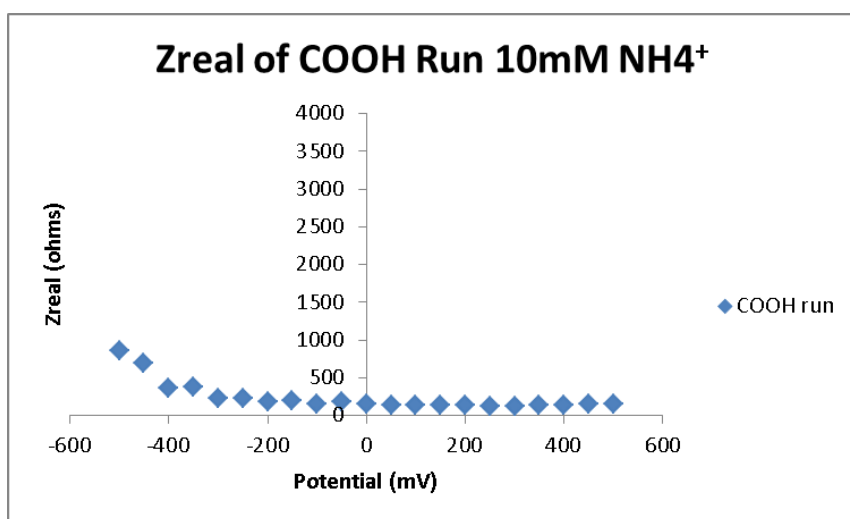
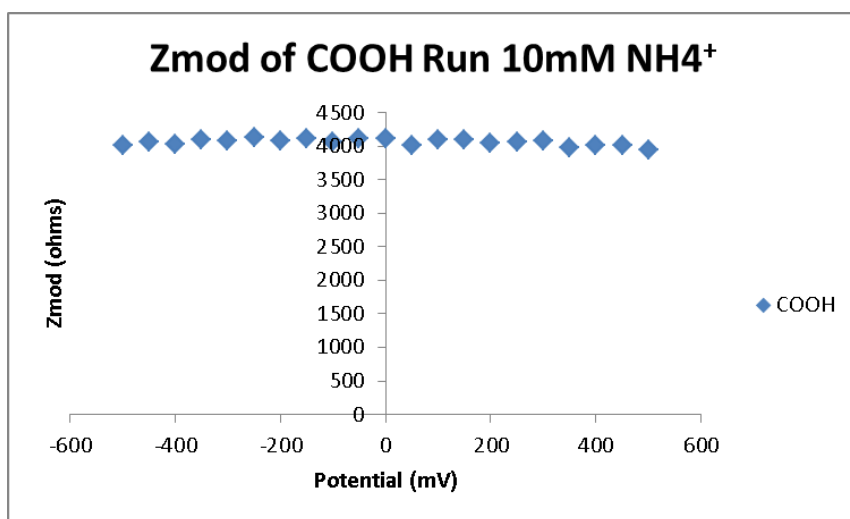


Figure 3.15: Z_{real} of COOH thiol surface EIS in the presence of 10mM NH_4^+ and Potassium ferricyanide redox probe



Graph 3.16: Z_{mod} of COOH thiol surface EIS in the presence of 10mM NH_4^+ and Potassium ferricyanide redox probe

3.9: CV of Potassium Ferricyanide

To determine the exact value of the reduction potential of Potassium ferricyanide, a Cyclic Voltammetry scan was made using a clean gold slide (**figure 3.17**). The scan limits were from -500mV to 500mV with a step size of 1mV. The area of the gold surface was 1cm². After analysis the redox potential was determined to be ~164 mV vs. Ag/AgCl ref. The literature value was 228.96 ± 0.01mV. (Taurino et al, 2011)

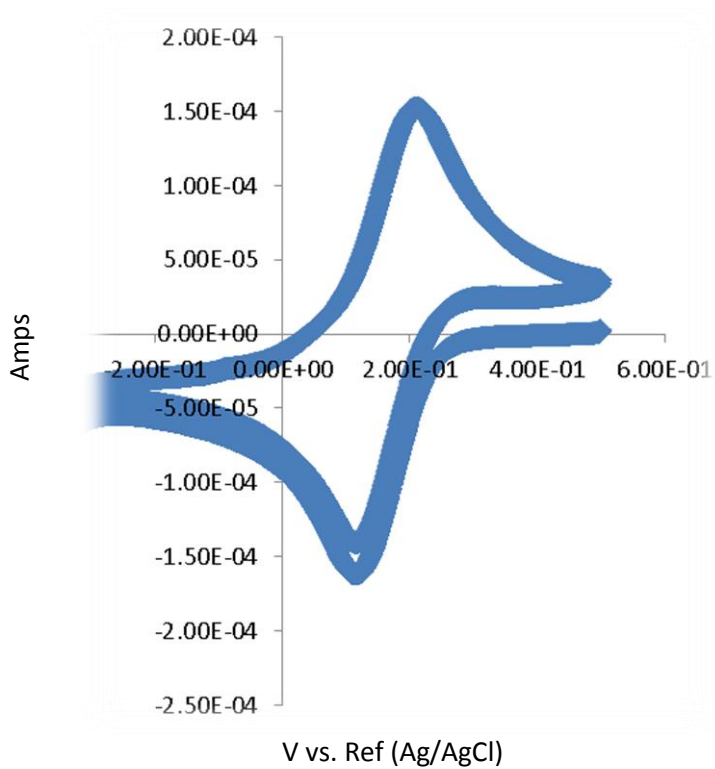


Figure 3.17: CV of Potassium Ferricyanide solution

Chapter 4: Discussion

This section aims to give a look into the data collected by each experiment and give the reader some meaning behind this data. This section also delves into seeing how the data supports or rejects the theory at hand and suggests future work that could be done.

4.1: EIS Results and Discussion

The purpose of these experiments was to determine the potential at which one could see the largest difference between the potassium and metal ions. Two redox probes were tested as well as a solution with no redox probe. After testing was complete, it was determined that the potassium ferricyanide redox probe showed the greatest difference in impedance. The potentials that seemed to show this difference were at 200 mV for Ammonium ions and -150 mV for potassium ions as shown in **figure 3.4** and **figure 3.5**. Also looking at these graphs, you will see that the frequencies chosen were 15.8 Hz and 9.93 Hz respectfully. The reason why these points were selected is because when trying to determine ammonium impedance, the potassium solution behaves the same as if there was neither ion in the solution at that frequency. This is also true when you are trying to determine the potassium impedance with -150 mV current at 9.93 Hz. Therefore if the potassium solution is acting as if there are no ions in the solution, it would be very easy to determine the ammonium impedance and vice versa.

4.2: Ion titrations Results and Discussion

The titration of the ions was the next step in the research. In doing this, graphs were made to show the change in Z_{phz} as the concentration of the ion went from 0 to 10 (**figures 3.6** and **3.7**). As you can see from these graphs, the Z_{phz} tended to increase as the concentration of the ions increased, with the Z_{phz} of the ammonium titration going from $\sim -75^\circ$ to $\sim -30^\circ$ and the potassium titration from $\sim -68^\circ$ and plateauing at $\sim -50^\circ$. Unfortunately the results of these titrations do not match what was predicted from the EIS graphs (**Figures 3.4** and **3.5**).

According to the EIS graphs, the Z_{phz} should have started out high and gradually decreased as the concentration of the ion increased. It is not quite understood what is happening on a molecular level during these titrations. However, what is seen is a change in the properties of the electrochemical cell due to the increase in the ion concentration. This could be due to how the ion already present in the solution is interacting with the 18-crown-6 surface and how the titrated ion interferes with these interactions as it is gradually added. These results lead to the belief that a new ionophore with a higher selectivity is needed to differentiate these ions.

4.3: EIS of NH₂ and COOH Thiol SAMs Results and Discussions

To better understand what is happening to the impedance of the electrochemical cell during the deprotonation of the ammonium ion, two different SAMs were tested; 11-mercaptoundecanoic acid and 11-amino-1-undecanethiol. These two compounds were put on gold surfaces and EIS was run. From the EIS measurements, graphs were made depicting the impedance of the electrochemical cell over the range of potentials. As you can see by the graphs, there are large spikes in Z_{phz} when using either potassium ferricyanide or Hexaamineruthenium(III) Chloride as the redox probes. The most interesting graphs are those measuring Z_{phz} . The Z_{phz} peaks at 150 mV when using the ferricyanide redox probe, and peaks at -150 when using the ruthenium(III) redox probe. When EIS is done without a redox probe, the Z_{phz} stays relatively level throughout the potentials which illustrates the necessity of a redox probe during these experimentations.

To test if these large increases in Z_{phz} is due to the reduction of the SAM compounds, a CV was done to test the redox potential of potassium ferricyanide. As shown in **figure 3.8**, two major peaks are visible (the minimum and maximum). The redox potential is calculated by taking the average potentials at these two peaks. The redox potential determined

was 164 mV. This is roughly the potential where the Z_{phz} peak is on the potassium ferricyanide run (**figure 3.8**). In addition the literature value for hexamineruthenium(III) chloride is -155mV. (Krysiński et al., 2002) This is the potential where the Z_{phz} peaked for the ruthenium run (**figure 3.10**). With both increases in Z_{phz} at the reduction potential of the redox probes present in solution, it is believed that the large spikes in Z_{phz} are due to the deprotonation of the SAM molecules.

One interesting issue about the CV of the potassium ferricyanide is how the results greatly differ from the known value of the reduction potential of the redox probe (~228mV). The reason for this shift is unknown and further testing needs to be done.

4.4: Difficulties and Recommendations for further study

This technology offers the possibility of monitoring ammonium ions in the presence of potassium ions and vice versa, but there are a few problems that need to be sorted before any prototype could be devised. One of these problems is with the relatively low selectivity of the commercially available ionophors. A new compound may be needed to replace the crown ether studied. Another challenge faced during the course of this research is that a relatively small change to the potential of the electrochemical cell, leads to a very large change to how the electrochemical cell reacts making it hard to predict the outcome of experiments. In addition, experimentation showed the necessity of having a redox probe present in solution. This makes the solution preparation more complex and therefore making the whole process more complex. These difficulties need to be address in later research.

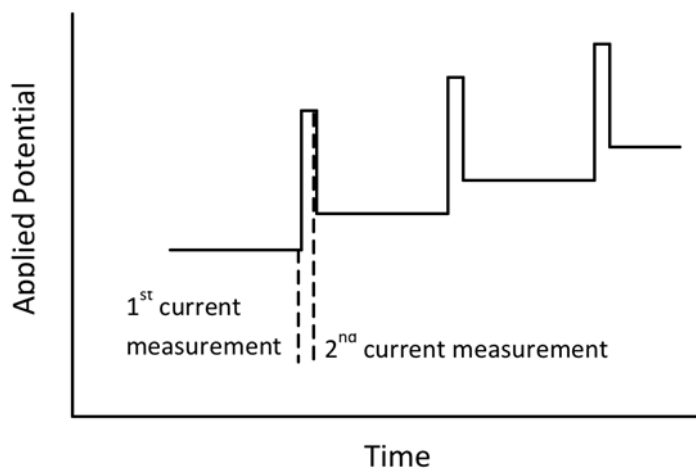


Figure 4.1: Differential Pulse Voltammetry Measurement

Differential pulse voltammetry is the next step to be taken in the progression of this technology. This is a technique used to study the redox properties of a very small amount of chemicals. To do this, a potential pulse is applied at regular intervals to the system and the current is measured right before and

right after each pulse. Normally the pulse is applied every 50 milliseconds and the current is calculated during the last 17 milliseconds of each pulse. (Encyclopedia Britannica Online)

Figure 4.1 shows an example of a differential pulse voltammetry measurement. In addition to differential pulse voltammetry, a new ionophore may be used to increase the ammonium/potassium ion selectivity of the sensor. Both of these steps need to be taken before a prototype can be made.

Chapter 5: Conclusions

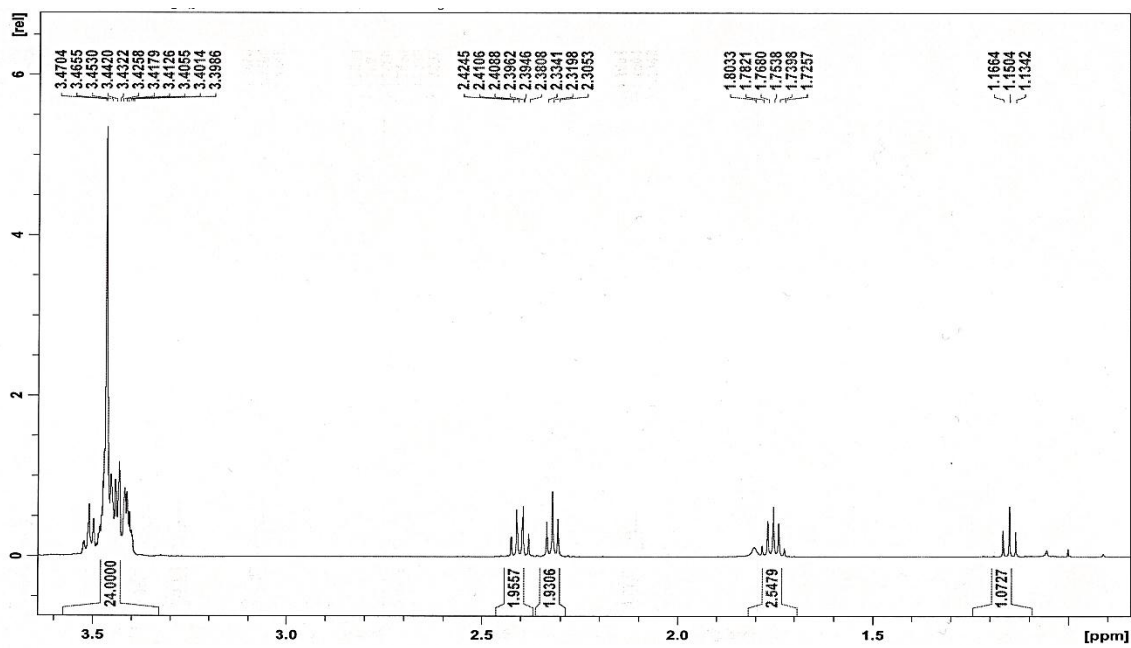
This paper presents the beginning stages in the development on a new Potassium/ammonium ion sensor. Using a controlled potential to improve the selectivity of the ionophors towards Potassium and ammonium ion detection promises to be a considerable improvement on current technology. There exists potassium ion sensors already in use but the main issue with this is that in the presence of ammonium ions the potassium concentration data becomes inaccurate. However, with an applied potential and in the presence of a reductive agent, the ammonium ion would lose a hydrogen group and thus change the electrochemical properties of the ion.

The main evidence of this is shown in the EIS graphs of the 18-crown-6 ether. With the potassium ferricyanide redox probe, there was a large separation between the two ions in the sense of Z_{phz} . These graphs (**Figures 3.4 and 3.5**) show that one could use the 18-crown-6 surface to measure for either ion depending on the potential applied; 200mV for Ammonium ions and -150mV for potassium ions. Unfortunately the ion titrations show a discontinuity in the data. Both Ion titration graphs show an increase in Z_{phz} which goes against the EIS graphs. It is unknown why this change occurred. The selectivity of the ionophors chosen may be a key issue in differentiating the two ions. Synthesizing an 18-crown-6 compound with bulkier groups could improve the selectivity for potassium ions. The bulky groups may be able to orient the crown in a vertical direction making the surface more rigid allowing the ring size to stay fixed. (Suzuki et al., 2000)

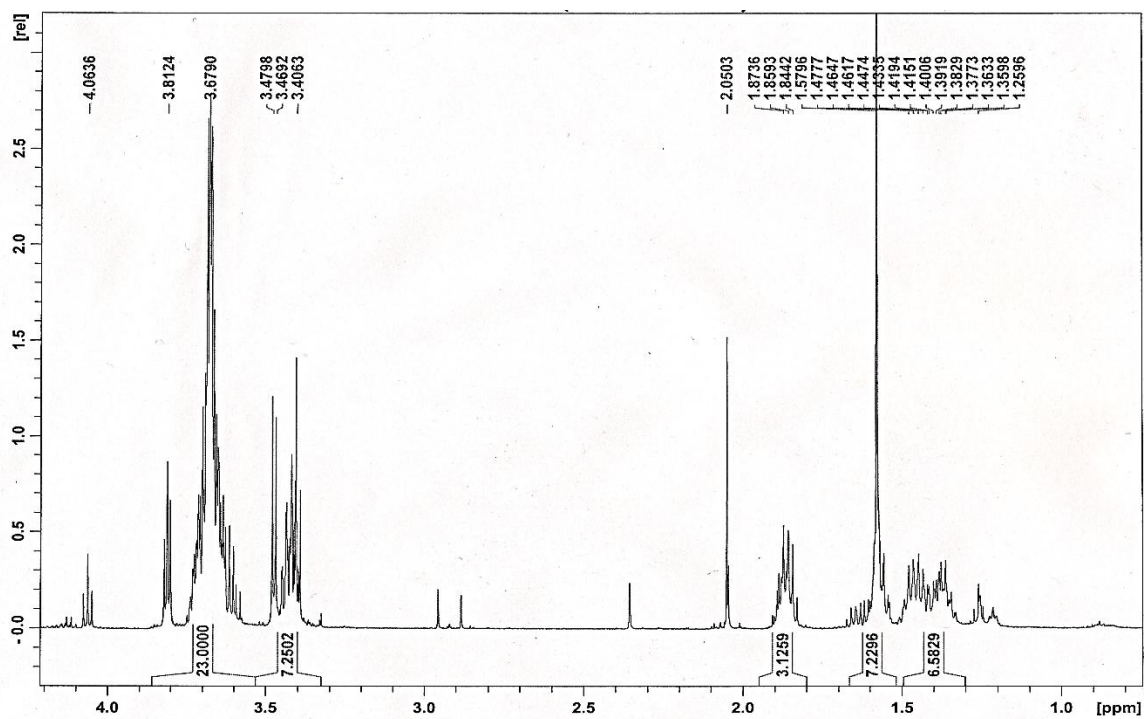
This technology looks promising for the development of a more selective sensor but more research needs to be done before any prototype can be developed. Selectivity of the ionophors is the main issue. Things to consider when deciding about a new ionophore are the chain length, crown size, and the addition of bulky groups on the crown to make the surface

more rigid. (Grady, 2010) In addition, the pH and temperature dependency of the electrochemical cell need to be tested. The pH of a tetra-n-butylammonium chloride solution is about 9 so the pH may need to be neutralized in order to increase selectivity of the ionophore. Work still remains to simplify the measurement technique so that sample preparation is minimized and to determine the absolute selectivity of the device. With a higher selectivity of the ionophore, this sensor could be a vast improvement over current technology in the accuracy of ammonium and potassium ion measurements.

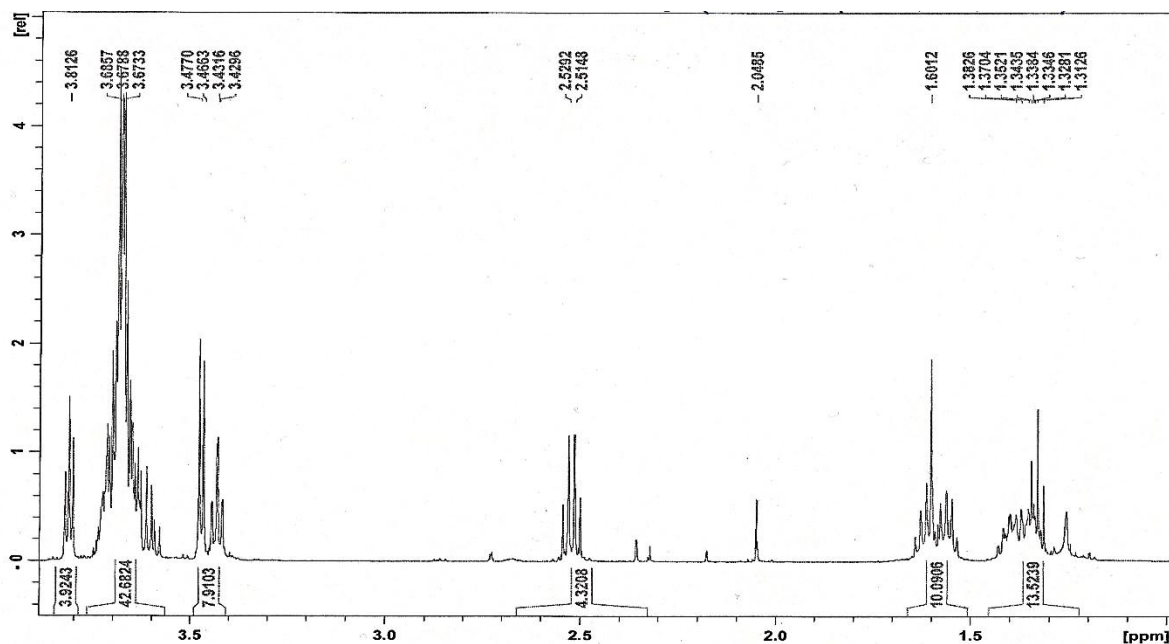
Appendix A: NMR Spectra



4-mercapto-1-(1,4,7,10,13-pentaoxa-16-azacyclooctadecan-16-yl)butan-1-one



2-(6-bromohexyloxy)methyl-18-crown-6



2-(6-mercaptohexyloxy)methyl-18-crown-6

Appendix B: References

- Andrienko, Denis. "Cyclic Voltammetry." (2008). 22 Jan. 2008. Web. 15 Apr. 2012.
<http://www.mpip-mainz.mpg.de/~andrienk/journal_club/cyclic_voltammetry.pdf>.
- Anslyn, Eric V. "Supramolecular Analytical Chemistry." *The Journal of Organic Chemistry* 72.3 (2007): 687-99. Print.
- Bigelow, W. C. (1946). *J. Colloid Interface Sci.*, 1, p. 513.
- Driscoll, Peter F. *Bioanalytical Applications of Chemically Modified Surfaces*. Diss. Worcester Polytechnic Institute., 2009. Print.
- Encyclopedia Britannica Online, s. v. "chemical analysis," accessed April 23, 2012,
<http://www.britannica.com/EBchecked/topic/108529/chemical-analysis>.
- Flink, S.; Boukamp, B. A.; van den Berg, A.; van Veggel, F. C. J. M.; Reinhoudt, D. N.,
Electrochemical detection of electrochemically inactive cations by self-assembled monolayers of crown ethers. *J. Am. Chem. Soc.* 1998, 120, (19), 4652-4657.

- Flink, S.; Van Veggel, F. C. J. M.; Reinhoudt, D. N., Recognition of Cations by Self-Assembled Monolayers of Crown Ethers. *J. Phys. Chem. B* 1999, 103, (31), 6515-6520.
- Gamry Instruments. "A Snapshot of Electrochemical Impedance Spectroscopy." Gamry Instruments. 2011. Web. 8 Apr. 2012. <http://www.gamry.com/assets/Application-Notes/A-Snapshot-of-EIS.pdf>
- Gamry Instruments. "Basics of Electrochemical Impedance Spectroscopy." Gamry.com. 3 Sept. 2010. Web. 26 Apr. 2012. <<http://www.gamry.com/assets/Application-Notes/Basics-of-EIS.pdf>>
- Gokel, George W., W. Matthew Leevy, and Michelle E. Weber. "Crown Ethers: Sensors for Ions and Molecular Scaffolds for Materials and Biological Models." *Chemical Reviews* 104.5 (2004): 2723-750. Print.
- Grady, William. Ionophore Analysis of 1-Aza-18-crown 6-Ether Using an Ion Selective Electrode. Worcester Polytechnic Institute, 28 Apr. 2010. Web. 26 Apr. 2012. <<http://www.wpi.edu/Pubs/E-project/Available/E-project-042710-115434/unrestricted/mqp%5B1%5D.pdf>>
- Grysakowski, B., J. Jasielec, B. Wierzba, T. Sokalski, A. Lewenstam, and M. Danielewski. "Electrochemical Impedance Spectroscopy (EIS) of Ion Sensors: Direct Modeling and Inverse Problem Solving Using the Nernst–Planck–Poisson (NPP) Model and the HGS(FP) Optimization Strategy." *Journal of Electroanalytical Chemistry* 662.1 (2011): 143-49. Print
- Hewage, Himali Sudarshani. *Studies of Applying Supramolecular Chemistry to Analytical Chemistry*. Diss. University of Texas at Austin, 2008. Print.
- Krysiński, Paweł, Agnieszka Żebrowska, Barbara Pałys, and Zenon Łotowski. "Spectroscopic and Electrochemical Studies of Bilayer Lipid Membranes Tethered to the Surface of Gold." *Journal of The Electrochemical Society* 149.6 (2002): E189. Print.
- Netzer, L.; Iscovici, R.; Sagiv, J., Adsorbed monolayers versus Langmuir-Blodgett-174 - monolayers - why and how? I. From monolayer to multilayer, by adsorption. *Thin Solid Films* 1983, 99, (1-3), 235-41.
- Netzer, L.; Iscovici, R.; Sagiv, J., Adsorbed monolayers versus Langmuir-Blodgett monolayers - why and how? II. Characterization of built-up films constructed by stepwise adsorption of individual monolayers. *Thin Solid Films* 1983, 100, (1), 67-76.
- Netzer, L.; Sagiv, J., A new approach to construction of artificial monolayer assemblies. *J. Am. Chem. Soc.* 1983, 105, (3), 674-6.
- New Scientist 1983, 98, 20.
- Nuzzo, R. G.; Allara, D. L. *J. Am. Chem. Soc.* 1983, 105, 4481.

- Park, Su-Moon, and Jung-Suk Yoo. "Peer Reviewed: Electrochemical Impedance Spectroscopy for Better Electrochemical Measurements." *Analytical Chemistry* 75.21 (2003): 455 A-61 A. Print.
- Sluytersrehabach, M. *Pure and Applied Chemistry*, 66 (1994), pp. 1831–1891
- Sondag-Huethorst, J. A. M.; Fokkink, L. G. J., *Electrochemical Characterization of Functionalized Alkanethiol Monolayers on Gold*. *Langmuir* 1995, 11, (6), 2237-41.
- Suzuki, Koji, Dwi Siswanta, Takeshi Otsuka, Tsuyoshi Amano, Takafumi Ikeda, Hideaki Hisamoto, Ryoko Yoshihara, and Shigeru Ohba. "Design and Synthesis of a More Highly Selective Ammonium Ionophore Than Nonactin and Its Application as an Ion-Sensing Component for an Ion-Selective Electrode." *Analytical Chemistry* 72.10 (2000): 2200-205. Print
- Taurino, Irene, Sandro Carrara, Mauro Giorcelli, Alberto Tagliaferro, and Giovanni De Micheli. "Comparison of Two Different Carbon Nanotube-based Surfaces with Respect to Potassium Ferricyanide Electrochemistry." *Surface Science* (2011). Print
- Ulman, A.; *Formation and Structure of Self-Assembled Monolayers*. *Chemical Reviews* 1996 96 (4), 1533-1554
- Wang, Hua, Shengfu Chen, Lingyan Li, and Shaoyi Jiang. "Improved Method for the Preparation of Carboxylic Acid and Amine Terminated Self-Assembled Monolayers of Alkanethiolates." *Langmuir* 21.7 (2005): 2633-636. Print
- Yang, Xinhao, J. Justin Gooding, D. Brynn Hibbert, and Naresh Kumar. "ChemInform Abstract: Synthesis of N-(3-Mercaptopropanoyl)-aza-18-crown-6, N-(4-Mercaptobutanoyl)-aza-18-crown-6 and Their Dimers." *ChemInform* 31.3 (2000). Print